

The Handedness of DNA Assembly around Carbon Nanotubes Is Determined by the Chirality of DNA

Published as part of *The Journal of Physical Chemistry* virtual special issue "Peter J. Rossky Festschrift".

Gül H. Zerze, Frank H. Stillinger, and Pablo G. Debenedetti*



Cite This: *J. Phys. Chem. B* 2020, 124, 5362–5369



Read Online

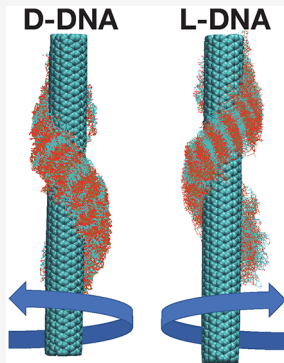
ACCESS |

Metrics & More

Article Recommendations

Supporting Information

ABSTRACT: Single-stranded DNA chains enable postsynthesis sorting of single-walled carbon nanotubes (CNTs) according to their diameter and helicity by wrapping helically around CNT surfaces. Both DNA chains and CNTs in these CNT–DNA conjugates are intrinsically chiral. Using a single-stranded DNA chain in both of its chiral realizations, we systematically study cross-chiral interactions between DNA and CNTs by varying the helicity of CNTs within a relatively narrow range of diameters. We find that regardless of the helicity or handedness of the carbon nanotube, the chirality of DNA dictates the handedness of its predominant helical wrap around carbon nanotubes.



INTRODUCTION

Single-walled carbon nanotubes (referred to as CNTs hereafter) are quasi-one-dimensional carbon nanomaterials employed in a wide range of bio- and nanotechnological applications owing to their unique chemical and physical properties.^{1–4} The structure of a CNT is defined by a lattice vector (n, m) that determines its diameter and helicity around its longitudinal axis. This helicity is quantified by a helical angle, α (Figure 1A), which has a range of possible values between -30° and $+30^\circ$ (Figure 1B). This helicity makes CNT structures chiral, except for lattice vectors of $n = m$ (armchair, $\alpha = 30^\circ$) or $m = 0$ (zigzag, $\alpha = 0^\circ$). The helical angles of (n, m) and (m, n) CNTs have the same magnitude but the opposite sign. Accordingly, we refer to (n, m) and (m, n) CNTs as having the same helicity but opposite handedness, following the terminology introduced by Zheng and co-workers.⁵

The properties of CNTs, such as thermal conductivity^{6,7} or current carrying capacity (ranging from metallic to semiconducting behavior),⁸ are a function of their structure, which is described by their lattice vector. A large-scale synthesis of CNTs, however, yields a mixture of various helicities and diameters (with either handedness). Therefore, postproduction processes to sort CNT mixtures according to their structure are necessary in order to be able to use CNTs for a particular application. A popular method, the use of surfactants, not only effectively disperses CNTs in an aqueous environment, but in addition, surfactants like single-stranded DNA can also form ordered wrapping structures on CNTs

with specific helicity and diameter, without affecting the CNTs' electrochemical properties. This specific binding enables chromatographic and aqueous two-phase purification of CNTs according to their helicity and diameter.^{5,9–11}

(GT)_n DNA sequences have been shown to assemble into a helical wrap around CNTs.⁹ Molecular dynamics (MD) simulations showed that DNA can spontaneously wrap around a CNT on nanosecond time scales¹² and free-energy surfaces show heterogeneity in the configurations that single-stranded DNA can assume on the CNT surface.¹³ A systematic search of a large library of DNA sequences has shown that specific DNA sequences have selectivity toward certain CNT helicities described by the lattice vector (n, m),¹¹ enabling the chromatographic purification of CNT mixtures according to their lattice vector. Some of the specific DNA sequence and CNT combinations found by the work of Zheng co-workers¹¹ have also been studied by MD simulations in order to understand the molecular origins of DNA's selectivity toward certain helicities of CNTs.^{14,15} The enantioselectivity of DNA sequences, however (i.e., their ability to differentiate between (m, n) and (n, m) CNTs), is a much less well-understood aspect of this picture. In an attempt to provide simultaneous

Received: March 30, 2020

Revised: May 31, 2020

Published: June 5, 2020



ACS Publications

© 2020 American Chemical Society

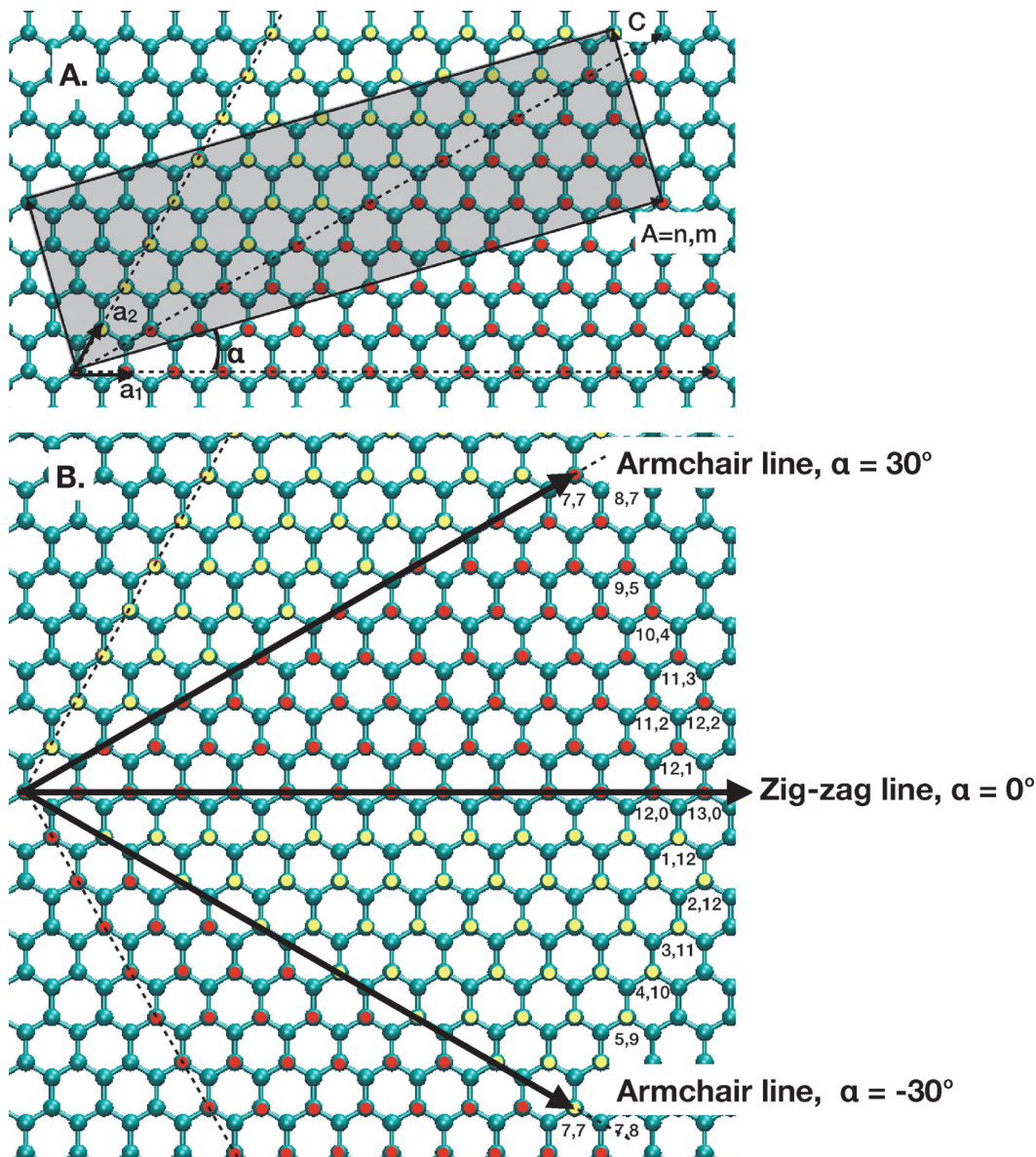


Figure 1. Schematic representation of graphene lattice vectors describing helicity and handedness of CNTs. (A) Radial projection of n, m CNT (this specific example is 10,4 CNT) with the perimeter given by the magnitude of vector A, and length given by the magnitude of vector C, where a_1 and a_2 are basis vectors and α is the helical angle, the angle between vector A and basis vector a_1 . (B) Schematic representation of the range of helical angles that CNTs can take (between two armchair lines).

helicity and handedness control, Zheng and co-workers showed that opposite handedness realizations of CNTs with the same helicity are functionally distinguishable in terms of their fluorescence emission intensity and chemical reactivity.⁵ The optical activity of DNA and chiral CNT conjugates has been detected via circular dichroism (CD).^{5,16} Replacing the DNA on the CNT surface with an achiral surfactant yielded a similar CD spectrum, indicating that the CD that CNT–DNA mixtures exhibit originates from the CNT's chirality, and not from DNA's chirality.⁵

Opposite-handed realizations of CNTs with the same magnitude of helical angle have experimentally been shown to be distinguishable by different DNA sequences⁵ and the energetics of this sequence-dependent recognition has been studied via a two-bead-per-nucleotide coarse-grained DNA model.¹⁷ Although some evidence in support of a possible energetic basis underlying the handedness of DNAs helical

wrap can be inferred from the two-bead-per-nucleotide model, which relies on B-DNA for torsional parameters, the model does not directly address the role of DNAs intrinsic chirality arising explicitly from carbon stereochemistry, which can potentially be used as an additional control parameter for simultaneous recognition of helicity and handedness. Nucleic acids are chiral due to the carbon stereocenters involved in the ribose (and deoxyribose) sugar moieties. The naturally occurring deoxyribose is D-deoxyribose, which possesses three stereocenters. All three stereocenters are inverted in L-deoxyribose. We note that nucleic acids possess no stereocenters other than the ones in ribose (or in deoxyribose). Accordingly, DNA chains with D-deoxyribose are referred to as D-DNA, whereas those with L-deoxyribose are referred to as L-DNA. While it is widely accepted that enantiomers of chiral molecules in achiral environments exhibit mirror image behavior,¹⁸ cross-chiral interactions in a chiral environment

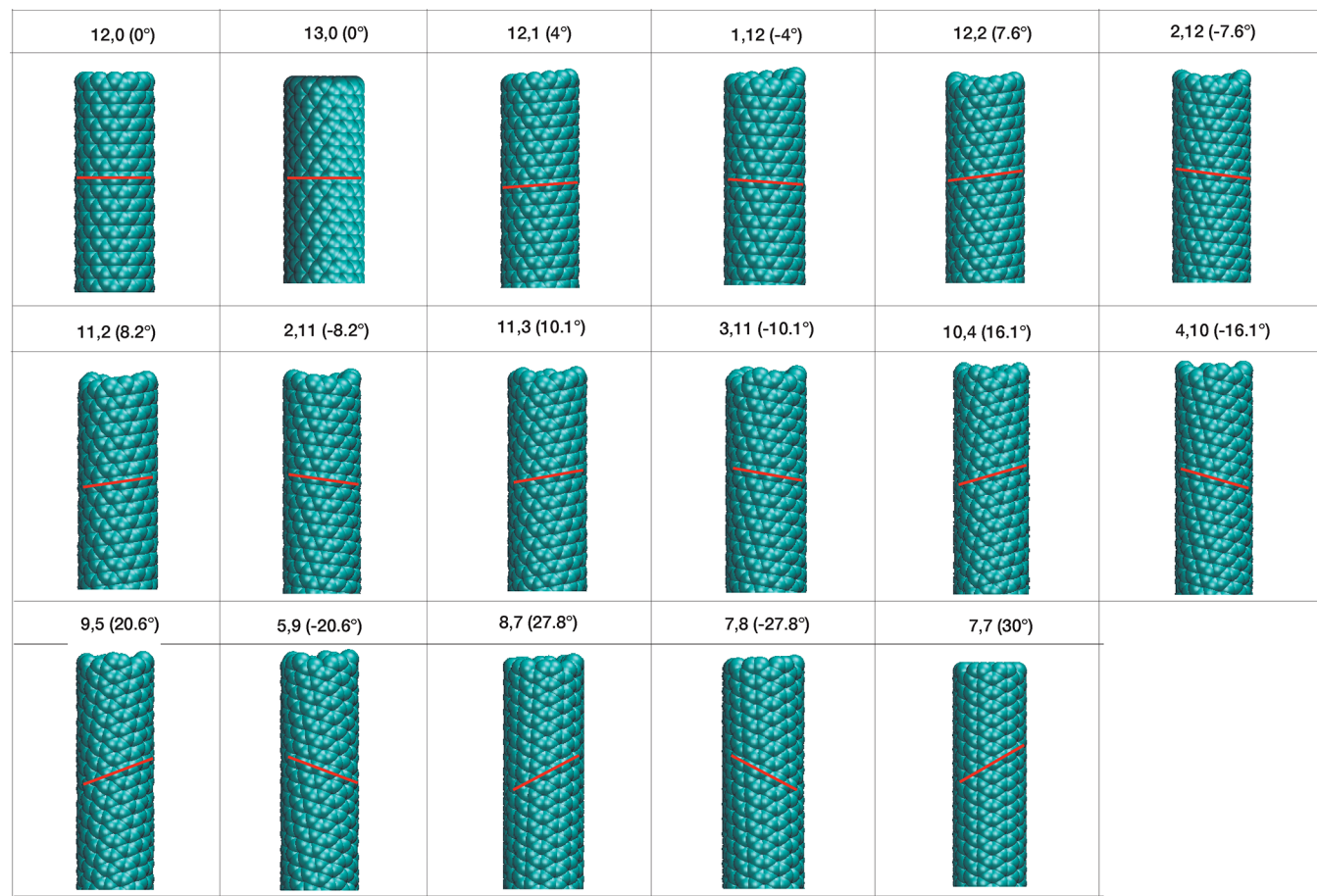


Figure 2. Graphical representations of all CNT helicities and handedness studied in this work. The helical angle of each CNT is given in parenthesis and calculated following eq 3 in the paper by Qin.¹⁹ The magnitude of the helical angle ranges between 0° and 30°, corresponding to zigzag and armchair CNTs, respectively.

might break this symmetry. Accordingly, in this work we systematically test the effect of DNA chirality on the wrapping properties around CNTs with various helicities and handedness and find that the chirality of the DNA determines the handedness of the predominant wrap around CNTs.

SIMULATION METHODS

The major parameter investigated in this work is the helical angle of the CNTs. Within a relatively narrow range of CNT diameter (1 ± 0.05 nm), we investigate all possible CNT helicities and handedness using the single-stranded DNA, (GT)_n. This diameter is selected since the average diameter of the commercial HiPco CNT product commonly used in experimental studies is around 1 nm.⁹ A DNA sequence of (GT)_n is selected as it provided the best separation of CNTs (of diameter around 1 nm) among a relatively small but systematic library of different DNA sequences studied by Zheng et al.⁹ Graphical representations of all CNTs studied in this work are given in Figure 2, together with their helical angles. For each CNT helicity and handedness, we separately study both the d-DNA and L-DNA, totaling 34 independent systems. We use the CHARMM36 force field, standard sp²-hybridized carbon parameters, and TIP3P water parameters to model DNA strands, CNT, and water, respectively. The chiralities of DNA and CNTs are imposed as initial conditions. We run parallel-tempering simulations to investigate equilibrium ensembles. Each simulation is run for 600 ns/replica.

Further modeling and sampling details are provided in the Supporting Information. We present the analysis of 300 K replicas excluding the initial 400 ns/replica as equilibration.

RESULTS AND DISCUSSION

We first analyze the adsorption of DNA on CNTs. In Figure S1, we show that all bases are adsorbed on CNT surfaces, within allowed fluctuation limits, in the 300 K ensembles of all CNTs. We then analyze the geometric properties of this adsorption. The handedness of a helical wrap around a CNT can be determined from the turn properties of individual nucleotides. We calculate whether a turn between residue i and $i + 1$ is right-handed or left-handed using the following metric: $\text{sgn}[(\vec{r}_i \times \vec{r}_{i+1}) \cdot \vec{n}] [(\vec{r}_{i+1} - \vec{r}_i) \cdot \vec{n}]$ where $\text{sgn}(x)$ is the sign function, given by $\text{d}x/\text{d}x$ for $x \neq 0$ and a value of +1 indicates a right-handed turn, whereas -1 indicates a left-handed turn. \vec{r}_i is a position vector with respect to the geometric center of the CNT in \mathbb{R}^3 , where i denotes residue index, and \vec{n} is a unit vector along the axial direction of the CNT. For each link between two successive residues, we determine the handedness of the turn as a function of time. For the position vector \vec{r}_i , we use the position of atom P for each residue, i . We exclude the first and last residue from the analysis, and we define a turn number i represents the link between residues $i + 1$ and $i + 2$, turn number $i + 1$ is the link between $i + 2$ and $i + 3$, and so on.

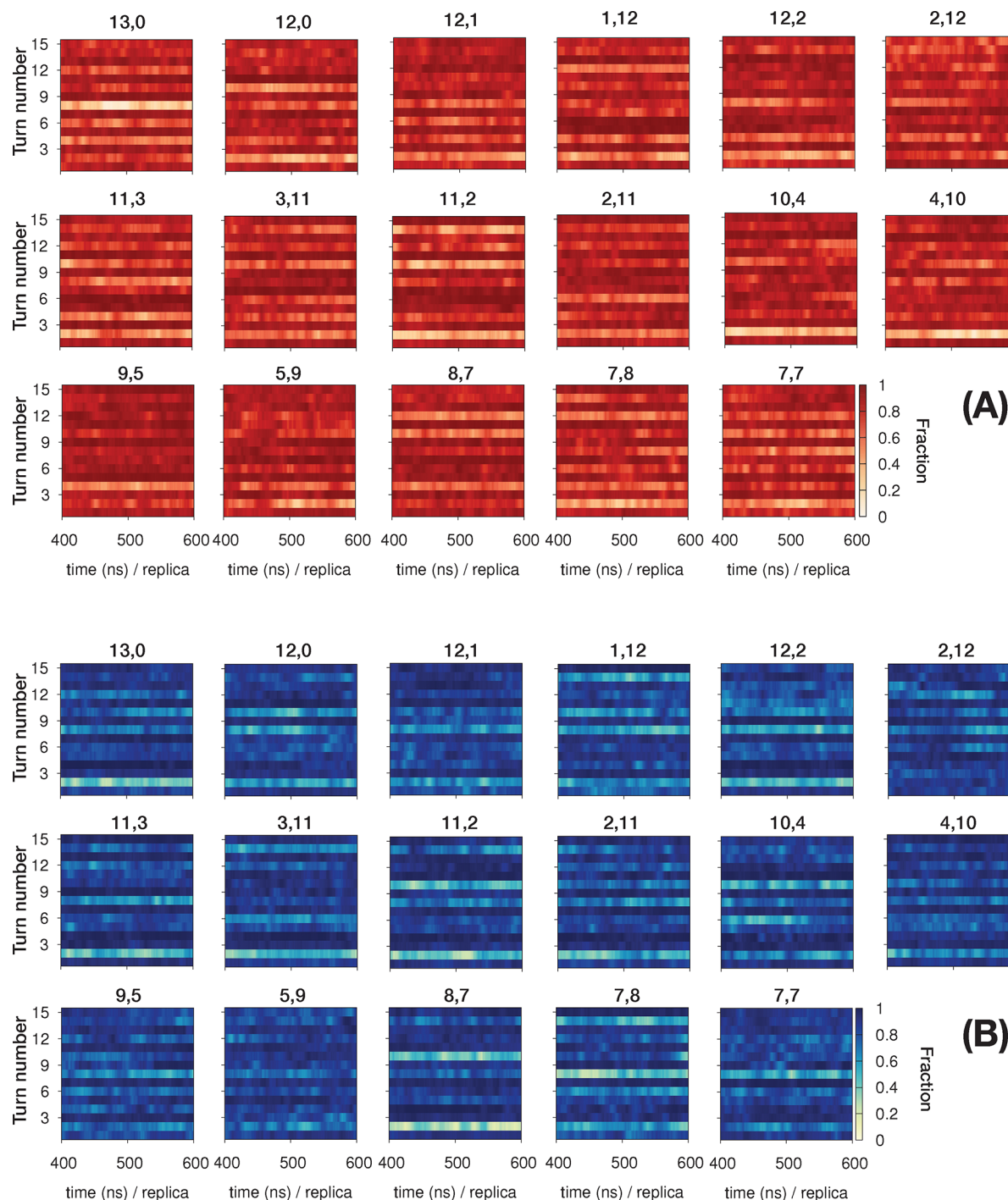


Figure 3. Average per-residue handedness of helical wraps of $(GT)_9$ around CNTs. (A) Fraction of the time d-DNA residues wrap around CNTs in a left-handed fashion. (B) Fraction of the time l-DNA residues wrap around CNTs in a right-handed fashion.

Relying on the analysis described above, we observe that links between d-DNA residues are predominantly left-handed turns resulting in an overall left-handed wrap around the CNT, whereas right-handed turns are predominant in l-DNA residues, resulting in an overall right-handed helical wrap, independent of the handedness or helicity of the CNT. In Figure 3, we show the fraction of time spent in a right-handed turn for each link for d-DNAs (A) and in a left-handed turn for each link for l-DNAs (B). The fraction is reported as a running average within 10 ns/replica blocks per link. As can be seen in each panel, the fraction of a particular handedness (left for d-

DNA, right for l-DNA) is almost always higher than 0.5; it rarely goes below 0.5 for any link, indicating that for DNA chains with d-sugars (d-DNA) the helical assembly is predominantly left-handed, whereas for l-DNAs, the resulting DNA assembly is predominantly right-handed. We note that mirror image systems should yield identical fractions of opposite-handedness helicity, such as left-handed helices of d-DNA on a (11,2) CNT and right-handed helices of l-DNA on a (2,11) CNT. While they look globally very similar, showing a distinct preference for opposite-handed helical wraps, there are some local differences between the time-

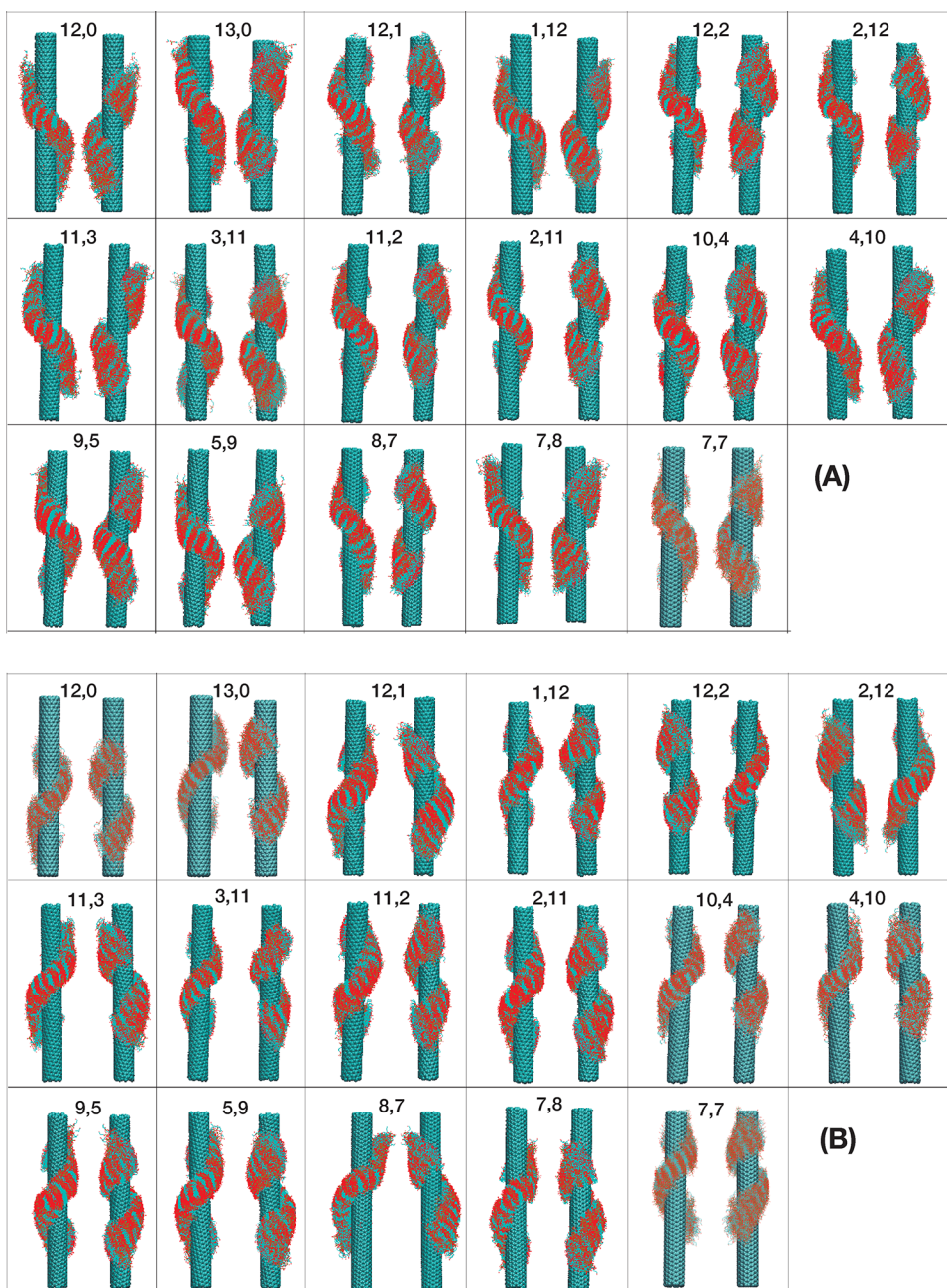


Figure 4. Clusters of contiguous helices of DNA on CNTs of different helicities and handedness for d-DNA (A) and for l-DNA (B). To ease the visualization of handedness of helical assemblies, only the backbone of DNA chains are illustrated together with CNTs and snapshots of assemblies are taken at two distinct view angles.

dependent handedness diagrams (top) and their corresponding mirror images (bottom) [e.g., 13,0 (top) vs 13,0 (bottom)], which are likely the result of statistical errors introduced by the finite length of the simulations. These local differences are more pronounced for even-numbered links (T to G). Interestingly, for all systems, odd numbered links have noticeably higher time fractions spent in left- or right-handed wrapping configurations compared to even-numbered links. As our systems are repeating units of GT (and we exclude the first and last residue from this analysis), all even-numbered links correspond to a turn between residue T and G, whereas all odd-numbered links correspond to a turn between residue G and T. This interesting finding will be subject of a future investigation of sequence specificity of helical assemblies.

To aid the visualization of the helical assemblies, we perform a clustering by imposing a helical contiguity criterion to the turn properties of surfactant DNAs. For each CNT–DNA combination, we collect all the configurations (at 300 K) where the turn between residues i and $i + 2$ has the same handedness for each even-numbered residue. We then remove the rotational and translational degrees of freedom by fitting these configurations to an arbitrarily selected configuration of this subpopulation (heavy atoms-only). The resulting clusters are presented in Figure 4 for each DNA–CNT conjugate, using two different view angles. It is clear that all contiguous helices are left-handed for d-DNAs (Figure 4A) whereas they are right-handed for l-DNAs (Figure 4B). The fraction of these contiguous helices is (on average) 0.48 (± 0.07) for all DNA–

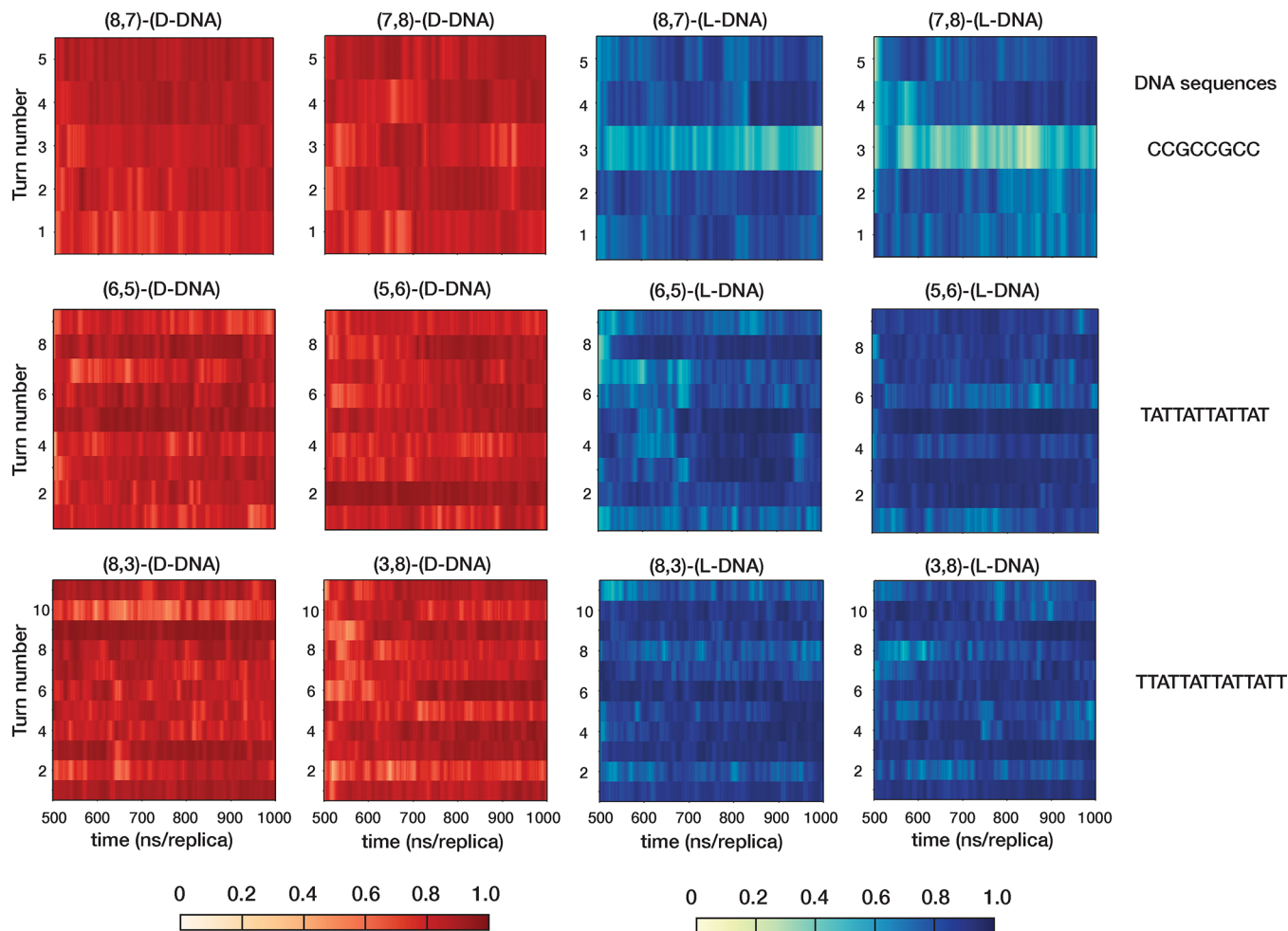


Figure 5. Fraction of the time that the DNA residues wrap around CNTs in a left-handed fashion (left panels, for D-DNAs) and in a right-handed fashion (right panels, for L-DNAs). The nucleotide composition of DNA chain on each separate CNT helicity is given on the right.

CNT combinations. The remaining configurations are still adsorbed on the surface and exhibit a large variation in their structures with loops and locally disrupted helices. We also calculate the pitch of these helical wraps as 4.9 ± 0.7 nm; we do not detect a statistically significant pitch sensitivity to CNT chirality. We emphasize that there does not exist any opposite-handed contiguous helical DNA assembly on any CNT (i.e., no left-handed contiguous helix for L-DNA and no right-handed contiguous helix for D-DNA).

As mentioned in the *Introduction*, some DNA sequences have been found to recognize specific CNTs in a CNT mixture.¹¹ We consider additional DNA–CNT combinations found to work by Zheng and co-workers,¹¹ including (6,5), (8,3), and (9,4) CNTs in combination with their specific DNA partners. These specific CNT–DNA pairs are selected by taking practical considerations into account: They contain some of the shortest sequences of DNA found in the work by Tu et al.,¹¹ allowing smaller system size and shorter simulation time requirements. We study both D-DNA and L-DNA on these CNTs and find that single-stranded DNA wraps around these CNTs helically, with a handedness again exclusively determined by DNA chirality (**Figure 5**). The helical wrapping of DNA on CNT surfaces has previously been identified by atomistic simulations,^{12–14} where the heterogeneity of helical-wrapping properties has been reported for specific DNA–CNT combinations. We note that we also observe a variety of DNA

configurations, including locally forming opposite-handed turns. However, these turns only disrupt the global handedness-preference of DNA's helical assembly locally.

The DNA sequence space is vast. Although we studied DNA sequences beyond $(GT)_9$, as described above, these additional sequences were still among the ones found to have the ability to bind selectively to nanotubes of specific helicities in CNT sorting studies.^{11,14} Therefore, we further extended our study to include a random DNA sequence of the same length as $(GT)_9$ on one of the achiral CNTs studied here (7,7). By random, we mean that the nucleotides at each position were randomly selected from four possible choices. Our results (**Figure S2**) indicated that the random DNA sequence also has a distinct handedness preference, depending solely on the chirality of the DNA. This is the same preference as exhibited by $(GT)_9$ and the other DNA sequences we studied here, namely, that D-DNA adopts left-handed and L-DNA adopts the mirror image right-handed wraps.

Klein and co-workers, using MD simulations, found that a D- $(GT)_{30}$ sequence adopted helical wraps on a (11,0) CNT, whose handedness depended on the starting configuration on the DNA.¹² These authors distinguished two DNA starting configurations by specifying average of backbone dihedral angles, one of which (named as S_1 with $\alpha = 260^\circ$, $\beta = 162^\circ$, $\gamma = 59^\circ$, $\delta = 140^\circ$, $\epsilon = 159^\circ$, $\zeta = 135^\circ$) spontaneously wrapped around the CNT in a right-handed fashion, whereas the other

(named as S_2 with $\alpha = 194^\circ$, $\beta = 116^\circ$, $\gamma = 62^\circ$, $\delta = 104^\circ$, $\epsilon = 143^\circ$, $\zeta = 216^\circ$) wrapped in a left-handed fashion. We note that our initial DNA configurations are not adsorbed, fairly extended configurations (Figure S3); i.e., they lack any particular bias toward a certain handedness. However, to be able to eliminate the possibility of such an initial condition dependence, we tested an additional DNA configuration that is analogous to the one labeled “ S_1 ” by Klein and co-workers,¹² by setting each backbone dihedral angle to a number equal to the average value used in ref 12. We only tested S_1 , as this was the DNA configuration that showed a spontaneous wrap with the opposite handedness with respect to our findings; i.e., Klein and co-workers found that S_1 wound around the CNT adopting a right-handed helix, despite being a D-DNA. In contrast, we show in Figure S4 that the D-(GT)₉ with initial backbone torsional angles identical to those of S_1 adopted a left-handed helical wrap on an achiral (7,7) nanotube. The L-(GT)₉ (with initial backbone torsions mirroring those of S_1) wrapped around the CNT via a right-handed helix. These observations rule out the possibility of an initial condition dependence in our calculations, in contrast to the observations by Klein et al.¹²

For the sake of computational simplicity, we consider rigid CNTs in most of this work (Supporting Information). In an effort to further generalize our conclusions, however, we repeat simulations of one of the DNA–CNT combinations ((GT)₉–7,7 CNT) both for L- and D-forms of DNA, while at the same time relaxing the CNT’s rigidity constraints. For this case, CNT bonds are kept flexible (using bond, angle, and torsion parameters given for standard sp^2 hybridized carbon in the CHARMM36 force field) and the rotational and translational displacements of the CNT are not restrained. Figure S5 shows the average per-residue handedness of helical wraps of both L- and D-forms of GT₉ around the flexible (7,7) CNT. We find that flexibility does not affect our conclusions about the preferred handedness. Moreover, we test a larger diameter CNT (15,15) CNT, 2 nm in diameter) with the same DNA sequence in order to see potential effects of CNT diameter on the handedness of DNA wrap around the CNT (Figure S6). We find that the diameter of CNT does not affect our conclusions about the preferred handedness, either.

As discussed by Klein and co-workers,¹³ each nucleotide experiences unique steric constraints associated with base adsorption, depending on the size of its base and that of its neighbors, which limits the system’s ability to adopt some configurations. While this might explain some of the residue-dependent differences we observe in fractions of particular handedness, it does not directly determine the mechanism underlying the handedness preference of the DNA sequences studied here, much less its dependence on the sugars’ chirality. Accordingly, our findings emphasize that some important global conformational properties of DNA helical assemblies arise not only from steric limitations caused by base adsorption but also from constraints driven by backbone (i.e., sugar) chirality.

In nature, when D-DNA chains hybridize forming a double-stranded helix, the predominant configuration is known to be a right-handed helix. We show that the mirror symmetry of carbon stereocenters in the DNA chain, i.e., a change from D-DNA to L-DNA, results in a mirror symmetry of the double-stranded helical configuration (Figure S7); i.e., L-DNA chains hybridize to form a left-handed double-stranded helix, as opposed to D-DNA. Interestingly, however, the handedness of

the respective (D- and L-) DNA chains wrapped around CNT has the opposite sign for all the cases studied in this work. Supramolecular DNA assemblies have recently been reported to show handedness opposite to that of their constituents (double-stranded DNA) as a function of deformation of helicities of the constituents²⁰ when helices are deformed by an externally imposed force (pulling). We are currently investigating the mechanisms underlying the contrasting chirality preferences involved in self-assembly on CNTs vs hybridization.

CONCLUSIONS

In this work, we systematically and specifically analyzed the helical properties of DNA–CNT assemblies. We found that helical assemblies of single-stranded DNA–CNT conjugates are insensitive to the helical properties of the CNTs. Instead, we consistently found that the chirality of the given DNA sequence determines the handedness of a helical wrap around CNTs. Although we observe local opposite-handed turns or local disruptions in helical assemblies (i.e., structural heterogeneity of the DNA strand wrapped on CNTs), when we impose a contiguity criterion, we find that a large fraction of DNA configurations adsorbed on CNTs form contiguous helices, which have a particular handedness. This handedness is solely a function of DNA’s chirality, and is insensitive to the range of CNT parameters or initial DNA configurations studied in this work. The DNA helicity-related quantities that we have calculated are not affected by CNT helicities and handedness in any statistically significant way. We note that our findings rely on a single DNA chain adsorbed on CNTs within a narrow range of diameters. Whether helical assemblies of multiple DNA strands on CNT surfaces spanning a broader range of diameters might be responsive to differences in CNT helicity and handedness will be the subject of future investigations.

ASSOCIATED CONTENT

SI Supporting Information

The Supporting Information is available free of charge at <https://pubs.acs.org/doi/10.1021/acs.jpcb.0c02816>.

Simulation details and figures of the normalized probability distribution, the average per-residue handedness of helical wraps, starting configurations, and comparison of the double-stranded helical structures (PDF)

AUTHOR INFORMATION

Corresponding Author

Pablo G. Debenedetti – Department of Chemical and Biological Engineering, Princeton University, Princeton, New Jersey 08544, United States;  orcid.org/0000-0003-1881-1728; Email: pdebene@princeton.edu

Authors

Gül H. Zerze – Department of Chemical and Biological Engineering, Princeton University, Princeton, New Jersey 08544, United States;  orcid.org/0000-0002-3074-3521

Frank H. Stillinger – Department of Chemistry, Princeton University, Princeton, New Jersey 08544, United States;  orcid.org/0000-0002-1225-8186

Complete contact information is available at:
<https://pubs.acs.org/10.1021/acs.jpcb.0c02816>

Notes

The authors declare no competing financial interest.

ACKNOWLEDGMENTS

G.H.Z. and P.G.D. acknowledge the support from Unilever R&D. The simulations presented in this work are performed on computational resources managed and supported by Princeton Research Computing, a consortium of groups including the Princeton Institute for Computational Science and Engineering (PICSciE) and the Office of Information Technology's High Performance Computing Center and Visualization Laboratory at Princeton University. G.H.Z. thanks Dr. Ming Zheng and Dr. Hasan Zerze for useful discussions.

REFERENCES

- (1) Gooding, J. J. Nanostructuring electrodes with carbon nanotubes: A review on electrochemistry and applications for sensing. *Electrochim. Acta* **2005**, *50*, 3049–3060.
- (2) Trojanowicz, M. Analytical applications of carbon nanotubes: a review. *TrAC, Trends Anal. Chem.* **2006**, *25*, 480–489.
- (3) Park, S.; Vosguerichian, M.; Bao, Z. A review of fabrication and applications of carbon nanotube film-based flexible electronics. *Nanoscale* **2013**, *5*, 1727–1752.
- (4) De Volder, M. F.; Tawfick, S. H.; Baughman, R. H.; Hart, A. J. Carbon nanotubes: present and future commercial applications. *Science* **2013**, *339*, 535–539.
- (5) Ao, G.; Streit, J. K.; Fagan, J. A.; Zheng, M. Differentiating left- and right-handed carbon nanotubes by DNA. *J. Am. Chem. Soc.* **2016**, *138*, 16677–16685.
- (6) Pop, E.; Mann, D.; Wang, Q.; Goodson, K.; Dai, H. Thermal conductance of an individual single-wall carbon nanotube above room temperature. *Nano Lett.* **2006**, *6*, 96–100.
- (7) Grujicic, M.; Cao, G.; Roy, W. N. Computational analysis of the lattice contribution to thermal conductivity of single-walled carbon nanotubes. *J. Mater. Sci.* **2005**, *40*, 1943–1952.
- (8) Niyyogi, S.; Hamon, M.; Hu, H.; Zhao, B.; Bhowmik, P.; Sen, R.; Itkis, M.; Haddon, R. Chemistry of single-walled carbon nanotubes. *Acc. Chem. Res.* **2002**, *35*, 1105–1113.
- (9) Zheng, M.; Jagota, A.; Strano, M. S.; Santos, A. P.; Barone, P.; Chou, S. G.; Diner, B. A.; Dresselhaus, M. S.; McLean, R. S.; Onoa, G. B.; et al. Structure-based carbon nanotube sorting by sequence-dependent DNA assembly. *Science* **2003**, *302*, 1545–1548.
- (10) Zheng, M.; Jagota, A.; Semke, E. D.; Diner, B. A.; McLean, R. S.; Lustig, S. R.; Richardson, R. E.; Tassi, N. G. DNA-assisted dispersion and separation of carbon nanotubes. *Nat. Mater.* **2003**, *2*, 338.
- (11) Tu, X.; Manohar, S.; Jagota, A.; Zheng, M. DNA sequence motifs for structure-specific recognition and separation of carbon nanotubes. *Nature* **2009**, *460*, 250.
- (12) Johnson, R. R.; Johnson, A. C.; Klein, M. L. Probing the structure of DNA-carbon nanotube hybrids with molecular dynamics. *Nano Lett.* **2008**, *8*, 69–75.
- (13) Johnson, R. R.; Kohlmeyer, A.; Johnson, A. C.; Klein, M. L. Free energy landscape of a DNA-carbon nanotube hybrid using replica exchange molecular dynamics. *Nano Lett.* **2009**, *9*, 537–541.
- (14) Roxbury, D.; Mittal, J.; Jagota, A. Molecular-basis of single-walled carbon nanotube recognition by single-stranded DNA. *Nano Lett.* **2012**, *12*, 1464–1469.
- (15) Shankar, A.; Mittal, J.; Jagota, A. Binding between DNA and carbon nanotubes strongly depends upon sequence and chirality. *Langmuir* **2014**, *30*, 3176–3183.
- (16) Dukovic, G.; Balaz, M.; Doak, P.; Berova, N. D.; Zheng, M.; McLean, R. S.; Brus, L. E. Racemic single-walled carbon nanotubes exhibit circular dichroism when wrapped with DNA. *J. Am. Chem. Soc.* **2006**, *128*, 9004–9005.
- (17) Shankar, A.; Zheng, M.; Jagota, A. Energetic basis of single-wall carbon nanotube enantiomer recognition by single-stranded DNA. *J. Phys. Chem. C* **2017**, *121*, 17479–17487.
- (18) Yashima, E.; Ousaka, N.; Taura, D.; Shimomura, K.; Ikai, T.; Maeda, K. Supramolecular helical systems: helical assemblies of small molecules, foldamers, and polymers with chiral amplification and their functions. *Chem. Rev.* **2016**, *116*, 13752–13990.
- (19) Qin, L.-C. Determination of the chiral indices (n, m) of carbon nanotubes by electron diffraction. *Phys. Chem. Chem. Phys.* **2007**, *9*, 31–48.
- (20) Tortora, M.; Mishra, G.; Presern, D.; Doye, J. P. Chiral shape fluctuations and the origin of chirality in cholesteric phases of DNA origamis. *arXiv:1811.12331* **2018**.